Available online at www.sciencedirect.com

ScienceDirect

Procedia Engineering 205 (2017) 1835–1842

Procedia Engineering

www.elsevier.com/locate/procedia

10th International Symposium on Heating, Ventilation and Air Conditioning, ISHVAC2017, 19-22 October 2017, Jinan, China

Outdoor and Indoor Ozone Concentration Estimation Based on Artificial Neural Network and Single Zone Mass Balance Model

Jialei Shen[a], Jie Chen[a], Xinyi Zhang[a], Sicong Zou[a], Zhi Gao[a,*]

[a]*School of Architecture and Urban Planning, Nanjing University, 22 Hankou Road, Nanjing, Jiangsu Province, 210093, China*

Abstract

Both outdoor and indoor ozone concentrations have negative health effects on human. This paper proposes an artificial neural network to estimate the outdoor ozone concentrations and a mass balance model tool to estimate indoor ozone concentrations. The prediction of outdoor and indoor ozone concentration levels is of great significance for people's health. The estimation models are validated by the measured data selected from the monitoring stations and field measurements in a room in Nanjing, respectively. The accuracy of the estimation models is evaluated. The neural network built in this paper can generally estimate the outdoor ozone concentrations to some extent, while the single zone mass balance model is useful for predicting indoor ozone concentration levels.

© 2017 The Authors. Published by Elsevier Ltd.
Peer-review under responsibility of the scientific committee of the 10th International Symposium on Heating, Ventilation and Air Conditioning.

Keywords: Ozone; Artificial neural network; I/O ratio; Deposition velocity;

1. Introduction

Ozone is a reactive gas that can adversely affect human health [1,2] and can cause damage to vulnerable materials [3]. Indoor residential ozone exposure accounts for 43%-76% of the total ozone exposure [4] since people usually spend on average almost 90% of their lives indoors [5,6,7,8]. Both outdoor and indoor ozone concentrations are closely associated with people's health. The estimation of ozone concentrations outdoors and indoors is therefore beneficial for preventing the health risks caused by ozone.

* Corresponding author. Tel.: +86-137-7641-8798.
E-mail address: zhgao@nju.edu.cn

1877-7058 © 2017 The Authors. Published by Elsevier Ltd.
Peer-review under responsibility of the scientific committee of the 10th International Symposium on Heating, Ventilation and Air Conditioning.
10.1016/j.proeng.2017.10.253

Artificial neural networks were considered as promising tools because of their simplicity towards simulation, prediction and modelling, of which back-propagation neural networks have been used to estimate outdoor pollutant concentrations by many previous studies. Feng et al. [9] proposed a hybrid back-propagation neural network to forecast PM2.5 pollutions in northern China. Bai et al. [10] developed a back-propagation neural network with wavelet transform model to forecast daily air pollutants (PM_{10}, SO_2, and NO_2) concentrations in China. Indoor ozone concentration levels are generally lower than outdoor levels due to irreversible reactions with indoor materials. Using a mass balance model in a well-mixed room, the indoor ozone concentration can then be estimated when indoor environment, materials and outdoor ozone concentration are known. Grøntoft and Raychaudhuri [11] developed the IMPACT model to make predictions of indoor concentration levels of some pollutant gases (O_3, SO_2 and NO_2) in museums. Walker and Sherman [12] estimated residential ozone levels using a single zone model.

This paper develops a back-propagation neural network to estimate the outdoor ozone concentrations and a mass balance model tool to estimate indoor ozone concentrations. The prediction of outdoor and indoor ozone concentration levels is of great significance for people's health. The estimation models are validated by the measured data selected from the monitoring stations and field measurements in a college student dormitory in Nanjing, respectively.

2. Methods

2.1. Neural network

The outdoor ozone concentrations are associated with the emission sources and the local meteorological parameters, including temperature (T), relative humidity (RH), wind velocity (U) and atmospheric pressure (P). However, the emission sources are related to many complicated factors. Thus this paper mainly focuses on the impacts of the local meteorological parameters on the outdoor ozone levels. Generally, the meteorological parameters and the pollutants levels, i.e. ozone (O_3) and nitrogen dioxide (NO_2), of one day will influence the predicted ozone level of the next day. Therefore, the meteorological parameters (T(d-1), RH(d-1), U(d-1), and P(d-1)) and the pollutants levels (O_3(d-1) and NO_2(d-1)) of one day, together with the fore-cast meteorological parameters of the next day (T(d), RH(d), U(d), and P(d)), are then used as the input variables for the next day's prediction of ozone levels (O_3(d)), i.e. 10 parameters in total. This paper collected totally 1210 sets of data of the daily meteorological parameters, ozone and nitrogen dioxide concentrations released by the monitoring stations in Nanjing (mean values of 9 monitoring stations). All data are partitioned into two subsets: 90% for training and 10% for testing.

A back-propagation neural network is chosen as the estimation model in this paper, which is built using the neural network toolbox in Matlab. The architecture of this neural network is shown in Fig. 1. The network consists of 1 input layer with 10 neurons (input variables), 1 hidden layer with 7 neurons, and 1 output layer with 1 neuron (output variable). Hyperbolic tangent sigmoid function (TANSIG) is used as the transfer function in hidden layer, while linear transfer function (PURELIN) is used as the transfer function in output layer. The Levenberg-Marquardt (LM) [13] algorithm is employed for training. The gradient descent with momentum weight and bias learning (GDM) algorithm is used as the adaption learning function.

The performance of the model is assessed by the mean relative error (MRE) and the root mean square error (RMSE), which are defined by

$$MRE = \frac{1}{N}\sum_{i=1}^{N}\left|\frac{E_i - M_i}{M_i}\right| \tag{1}$$

$$RMSE = \sqrt{\frac{1}{N}\sum_{i=1}^{N}(E_i - M_i)^2} \tag{2}$$

where N is the number of time points, and E_i and M_i represent the estimated and measured values.

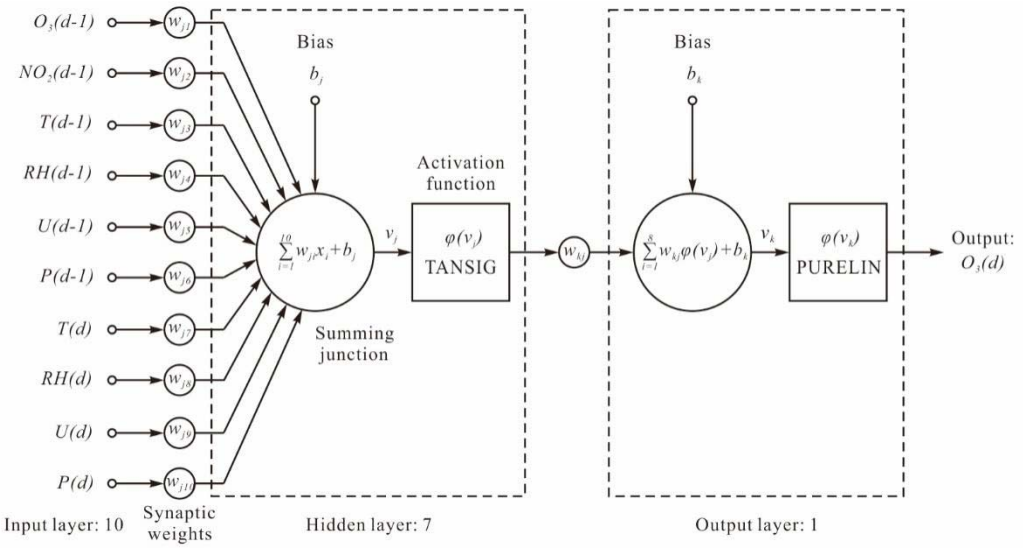

Fig. 1. The architecture of the back-propagation neural network.

2.2. Single zone mass balance model

The indoor ozone concentration estimations are based on a single zone mass balance model that depends on air flows in and out of the buildings [12]. The steady state indoor ozone concentration can be calculated by

$$C = \frac{\lambda C_o + S'/V}{\lambda + \left(\sum v_{d,i} A_i\right)/V} \tag{3}$$

where C is the indoor ozone concentration (mg/m^3), C_o is the outdoor ozone concentration (mg/m^3), S' is the ozone emission rate of indoor source (mg/h), V is the building volume (m^3), λ is the air change rate (h^{-1}), $v_{d,i}$ is the deposition velocity of the ith building surface material (m/h) and A_i is the area of the ith building surface (m^2). If $S' = 0$, then the equations are simplified as a condition without any indoor ozone source. The ozone deposition velocity to a surface encompasses the transport of ozone to the surface and the reactivity of a surface with ozone, which can be calculated by [14]

$$\frac{1}{v_d} = \frac{1}{v_t} + \frac{1}{v_s} = \frac{1}{v_t} + \frac{4}{\gamma \langle v \rangle} \tag{4}$$

where v_d is the deposition velocity (m/h), v_t is the transport-limited deposition velocity (m/h), v_s is the reaction-limited deposition velocity (m/h), γ is the reaction probability (-), which is the ozone removal rate divided by the ozone collision rate, and $\langle v \rangle$ is Boltzmann velocity for ozone ($\langle v \rangle = 3.60 \times 10^4$cm/s).

Values of v_d, v_t and γ from measurements made both in experimental chambers and in real rooms are reported in literatures. Table 1 compiles γ of common indoor materials from previous studies. The experimental results of Hoang et al. [15], Lamble et al. [16] and Gall et al. [17] suggested that the effects of temperature and humidity on γ are negligible. Thus, the value of γ of each material is treated as a constant in this paper. Values of γ vary over four orders of magnitude for typical indoor materials, from 10^{-8} (e.g. glass) to 10^{-5} (e.g. carpet and brick). A similar approach to Grøntoft and Raychaudhuri [11], value of γ of each material is mean of experimental measurement values from literatures. If the literature values are orders of magnitude different, the most improbable values will be discarded.

Values of v_t are determined by the indoor air flow condition, which depend on specific experimental or measured conditions. Values of v_t in an apartment were measured ranged from 0.1cm/s to 0.7cm/s [18]. Gall et al. [17] measured values of v_t in a room-scale chamber (5.5m×4.6m×2.7m) with different mixing conditions. Values of v_t range between 0.33cm/s for low mixing condition and 0.70cm/s for high mixing condition. Grøntoft and Raychaudhuri [11] set values of v_t in the range between 0.1cm/s and 0.75cm/s in the IMPACT model. This paper sets v_t in the range between 0.1cm/s and 0.7cm/s according to different indoor air flow conditions.

Table 1. Values of reaction probability (γ) for ozone.

Material	γ (-)	Material	γ (-)
Glass[11,14,19,20,26]	6.06E-08	Wall plaster, clay[16,28]	2.20E-05
Lucite[14]	5.50E-08	Sunflower[15]	3.78E-06
Metal, aluminum[11,14,19]	1.08E-07	Cork[15]	5.67E-06
Metal, stainless steel[11]	1.30E-06	Wheat[15]	5.22E-06
Metal, galvanized steel[19,21]	1.10E-06	Nylon[11,14]	5.50E-08
Ceramic[15]	4.44E-07	FEP Teflon[14]	5.50E-07
Stone material, soft dense[11]	7.82E-06	Rubber[16,26,28]	6.86E-06
Stone material, hard dense[11]	1.67E-08	Neoprene[14]	1.90E-06
Floor, wooden[24]	1.20E-06	Polyethylene sheet[14]	1.10E-06
Floor, finished hardwood[16,28]	2.45E-06	Medium density fiberboard[27]	4.50E-06
Floor, finished bamboo[16,28]	1.95E-06	Particle board[27]	5.00E-07
Porcelain clay tile[16,28]	1.02E-06	Plywood[11,14,19]	5.80E-07
Resilient tile[16,28]	1.11E-06	Bamboo[15]	4.44E-07
Ceiling tile, perlite[16,17,28,29]	1.02E-05	Cedar[26]	5.20E-06
Ceiling tile, mineral fiber[16,28]	4.65E-05	Woodwork, fine, hard[11]	5.59E-07
Ceiling tile, fiberglass[16,28]	3.74E-05	Woodwork, course, soft[11]	4.16E-06
Concrete, course[11]	9.65E-06	Cloth, <1 year old[11]	8.99E-06
Concrete, fine[11]	4.20E-06	Cloth, >1 year old[11]	7.06E-07
Wallpaper[11,19,20,26]	4.28E-06	Linoleum[11]	7.89E-07
Fabric wall covering[16,28]	5.30E-06	Linen[11,14]	6.30E-07
Paint, latex[16,19,20,28]	1.47E-06	Carpet, recycled[16,17,28,29]	3.20E-05
Paint, clay[16,28]	5.65E-05	Carpet, fabric-backed[16,28]	2.30E-05
Paint, water-based[26]	4.90E-06	Carpet, nylon[22,28,30]	1.38E-05
Paint, oil-based[26]	6.10E-06	Carpet, olefin[22,28,30]	1.01E-05
Paint, collagen[16,28]	3.15E-06	Carpet, wool[11]	1.06E-05
Gypsum board, painted[11,17,28,29,33]	4.72E-06	Brick[11]	1.59E-05
Gypsum board, untreated[11]	1.73E-05	Activated carbon cloth[11,25,28,29]	2.24E-05

2.3. Validation of the estimation

10% of the data of daily meteorological parameters, ozone and nitrogen dioxide concentrations released by the monitoring stations in Nanjing are used as the testing set of the neural network to validate the data estimated by the neural network. The indoor estimated results of the single zone mass balance model are validated by the field measurements conducted for a period of 37 days (July 15, 2015 to August 31, 2015) in a student dormitory without any indoor ozone source, which located in Nanjing University, China. Both indoor and outdoor ozone concentrations are measured at 1min interval by using the ozone monitors (2B Technologies, POM and Model 202). Air exchange rate (λ) of the room was evaluated according to the concentration decay of SF_6, which measured by Innova 1412i

Lumasense gas monitor. As shown in Fig. 2, the volume of the research room is 45m^3 (3m×5m×3m). The floor and ceiling are wooden and latex painted, respectively. All the walls are latex painted, of which two walls are covered with wallpapers. In addition, there are still some wooden furniture in the room.

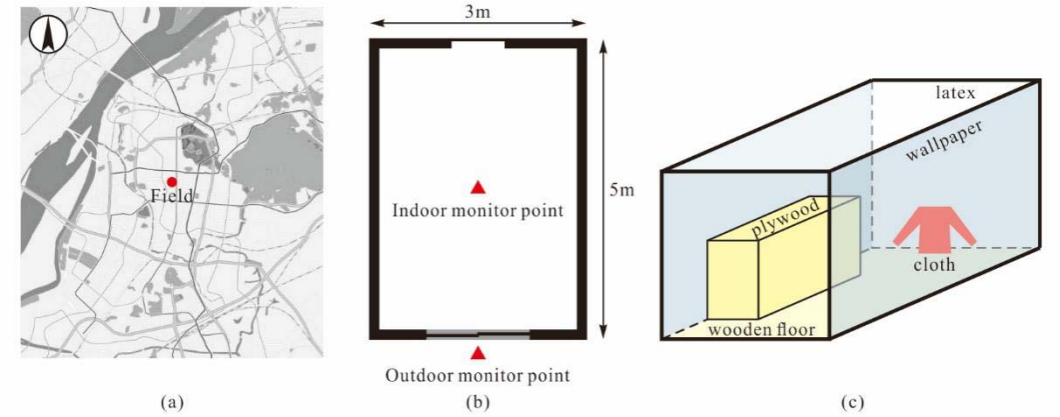

Fig. 2. (a) Location of field measurement, (b) monitor points, and (c) indoor materials.

3. Results

3.1. Outdoor ozone estimation based on artificial neural network

The best validation performance of the back-propagation neural network is at epoch 13. Fig. 3 shows the regression of estimated data and target data of training and validation sets. Fig. 4 illustrates the outdoor ozone concentrations estimated by the neural network and the testing data released by the monitoring stations in Nanjing. Generally, the estimated data are following the measured data. The RMSE of the estimated data is 22.5 and the MRE is 24.0%. Therefore, generally, the network built in this paper can estimate the outdoor ozone concentrations to some extent. More input data, together with some other variable, are required for improving the estimating results.

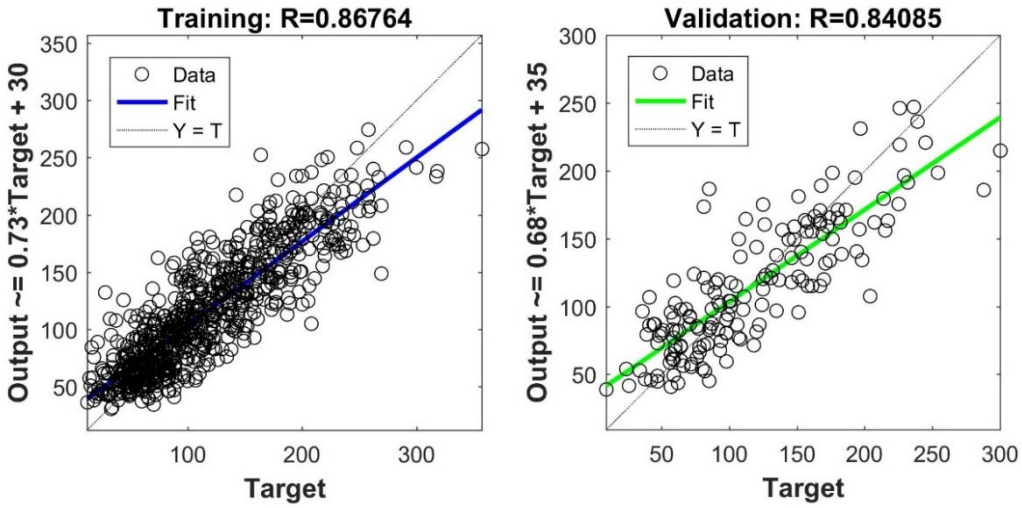

Fig. 3. Regression of estimated data and target data of training and validation subsets.

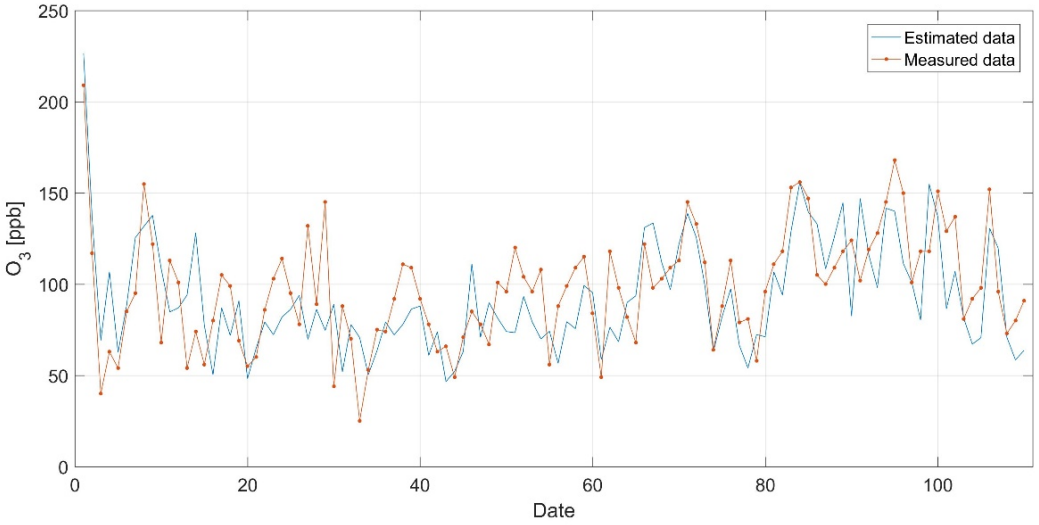

Fig. 4. Outdoor ozone concentrations estimated by the neural network and the measured data released by the monitoring station.

3.2. Indoor ozone estimation based on single zone mass balance model

Values of v_d, v_t and γ from measurements made both in experimental chambers and in real rooms are reported in the literatures, which are adopted by this study. The experimental results show that the air change rate of the research room is 1.32h^{-1} when the windows are open, and 0.66h^{-1} when the windows are closed. Value of v_d of each material in the room is calculated through Eq. (4) by assuming v_t is 0.5cm/s with the windows open and 0.3cm/s with the windows closed. The measured indoor and outdoor ozone concentrations of the research room with the windows open and closed are shown in Fig. 5(a) and 5(b), respectively. The measured data in Fig. 5(a) and 5(b) are mean values of monitoring for 1h, which is therefore considered to be steady state. The measured indoor/outdoor (I/O) ozone concentration ratios are 0.44 and 0.30, respectively. The estimated I/O ozone ratios are highly consistent with the measured ones, i.e. 0.49 and 0.33 respectively, which indicates the single zone mass balance model is useful for predicting indoor ozone concentration levels.

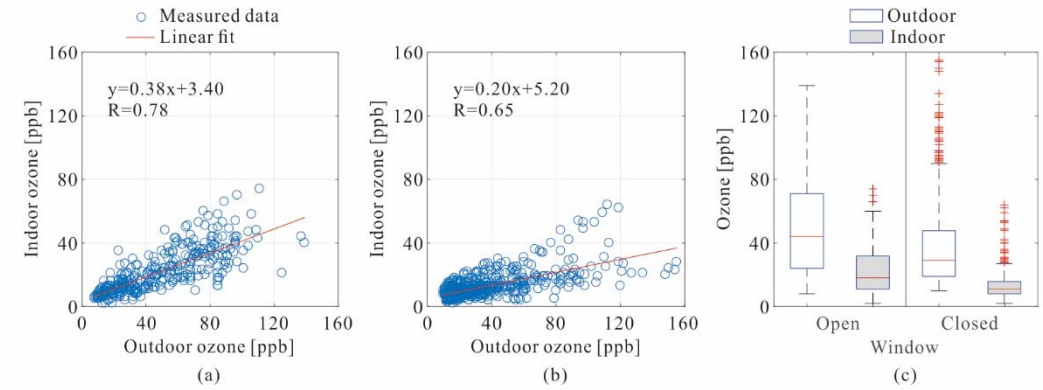

Fig. 5. The measured indoor and outdoor ozone concentrations of the research room with the windows (a) open and (b) closed. (c) Boxplots of measured ozone levels. In each box, the mid-line shows the median value, the top and bottom of the boxes show the upper and lower quartiles (the 75th and 25th percentiles), and the top and bottom of the whiskers represent the 90th and 10th percentiles. The extreme values farther from the median than 1.25 times the whisker end are drawn with markers.

4. Discussions

The neural network developed in this paper can generally estimate the outdoor ozone concentrations to some extent. The estimation accuracy of the back-propagation neural network is dependent on the training set. Thus more input data, together with more other variables, are required for improving the estimating results. The single zone mass balance model is useful for predicting indoor ozone concentration levels.

5. Conclusions

This paper proposes a back-propagation neural network to estimate the outdoor ozone concentrations and develops a mass balance model tool to estimate indoor ozone concentration levels. The prediction of outdoor and indoor ozone concentration levels is of great significance for people's health. The estimation models are validated by the measured data selected from the monitoring stations and field measurements in a room in Nanjing. The accuracy of the estimation models is evaluated. The back-propagation neural network built in this paper can generally estimate the outdoor ozone concentrations to some extent, while the single zone mass balance model is useful for predicting indoor ozone concentration levels.

Acknowledgements

The research was supported financially by the national key project of the Ministry of Science and Technology, China on "Green Buildings and Building Industrialization" through Grant No. 2016YFC0700500. Thanks are due to Vutrunghieu Nguyen for his help in field measurement.

References

[1] U.S. Environmental Protection Agency, An Office Building Occupant's Guide to Indoor Air Quality Office of Air and Radiation, Indoor Environments Division, Washington DC, 1997.
[2] M. Jerrett, R.T. Burnett, C.A. Pope, K. Ito, G. Thurston, D. Krewski, M. Thun, Long-term ozone exposure and mortality, N. Engl. J. Med. 360 (11) (2009) 1085–1095.
[3] N. Blades, T. Oreszczyn, B. Bordass, M. Cassar, Guidelines on pollution control in museum buildings, Museum Association, London, 2000.
[4] C. J. Weschler, Ozone's impact on public health: contributions from indoor exposures to ozone and products of ozone-initiated chemistry, Environ. Health Persp. 114 (10) (2006) 1489–1496.
[5] N.E. Klepeis, W.C. Nelson, W.R. Ott, J.P. Robinson, A.M. Tsang, P. Switzer, W.H. Engelmann, The National Human Activity Pattern Survey (NHAPS): a resource for assessing exposure to environmental pollutants, J. Expo. Anal. Env. Epid. 11 (3) (2001) 231–252.
[6] B.R. deCastro, S.N. Sax, S.N. Chillrud, P.L. Kinney, J.D. Spengler, Modeling time-location patterns of inner-city high school students in New York and Los Angeles using a longitudinal approach with generalized estimating equations, J. Expo. Sci. Env. Epid. 17 (3) (2007) 233–247.
[7] C. Schweizer, R.D. Edwards, L. Bayer-Oglesby, W.J. Gauderman, V. Ilaqua, M. Juhani Jantunen, N. Künzli, Indoor time-microenvironment-activity patterns in seven regions of Europe, J. Expo. Sci. Env. Epid. 17 (2) (2007) 170–181.
[8] T. Hussein, P. Paasonen, M. Kulmala, Activity pattern of a selected group of school occupants and their family members in Helsinki-Finland, Sci. Total Environ. 425 (15) (2012) 289–292.
[9] X. Feng, Q. Li, Y. Zhu, J. Hou, L. Jin, J. Wang, Artificial neural networks forecasting of PM2.5 pollution using air mass trajectory based geographic model and wavelet transformation. Atmos. Environ. 107 (2015) 118–128.
[10] Y. Bai, Y. Li, X. Wang, J. Xie, C. Li, Air pollutants concentrations forecasting using back propagation neural network based on wavelet decomposition with meteorological conditions, Atmos. Pollut. Res. 7 (3) (2016) 557–566.
[11] T. Grøntoft, M.R. Raychaudhuri, Compilation of tables of surface deposition velocities for O3, NO2 and SO2 to a range of indoor surfaces, Atmos. Environ. 38 (4) (2004) 533–544.
[12] I.S. Walker, M.H. Sherman, Effect of ventilation strategies on residential ozone levels, Build. Environ.59 (2013) 456–465.
[13] A.J. Shepherd, Second-order Methods for Neural Networks, Springer, New York, 1997.
[14] J.A. Cano-Ruiz, D. Kong, R.B. Balas, W.W. Nazaroff, Removal of reactive gases at indoor surfaces: combining mass transport and surface kinetics, Atmos. Environ. 27 (1993) 2039–2050.
[15] C.P. Hoang, K.A. Kinney, R.L. Corsi, Ozone removal by green building materials, Build. Environ. 44 (2009) 1627–1633.
[16] S.P. Lamble, R.L. Corsi, G.C. Morrison, Ozone deposition velocities, reaction probabilities and product yields for green building materials, Atmos. Environ. 45 (2011) 6965–6972.
[17] E. Gall, E. Darling, J.A. Siegel, G.C. Morrison, R.L. Corsi, Evaluation of three common green building materials for ozone removal, and primary and secondary emissions of aldehydes, Atmos. Environ. 77 (2013) 910–918.

[18] G.C. Morrison, Z. Ping, D.J. Wiseman, M. Ongwandee, H. Chang, J. Portman, S. Regmi, Rapid measurement of indoor mass-transfer coefficients, Atmos. Environ. 37 (2003) 5611–5619.
[19] D.L. Liu, W.W. Nazaroff, Modeling pollutant penetration across building envelopes, Atmos. Environ. 35 (2001) 4451–4462.
[20] R. Reiss, P.B. Ryan, P. Koutrakis, S.J. Tibbetts, Ozone Reactive Chemistry on Interior Latex Paint, Environ. Sci. Technol. 29 (1995) 1906–1912.
[21] G.C. Morrison, W.W. Nazaroff, J.A. Cano-Ruiz, T. Alfred, M.P. Modera, Indoor Air Quality Impacts of Ventilation Ducts: Ozone Removal and Emissions of Volatile Organic Compounds, J. Air Waste Manage. Assoc. 48 (1998) 941–952.
[22] G.C. Morrison, W.W. Nazaroff, The Rate of Ozone Uptake on Carpets: Experimental Studies, Environ. Sci. Technol. 34 (2000) 4963–4968.
[23] B.K. Coleman, H. Destaillats, A.T. Hodgson, W.W. Nazaroff, Ozone consumption and volatile byproduct formation from surface reactions with aircraft cabin materials and clothing fabrics, Atmos. Environ. 42 (2008) 642–654.
[24] C.C. Lin, S.C. Hsu, Deposition velocities and impact of physical properties on ozone removal for building materials, Atmos. Environ. 101 (2015) 194–199.
[25] T. Grøntoft, Dry deposition of ozone on building materials. Chamber measurements and modelling of the time-dependent deposition, Atmos. Environ. 36 (2002) 5661–5670.
[26] K. Ito, Experimental and CFD analyses examining ozone distribution in model rooms with laminar and turbulent flow fields, J. Asian Archit. Build. Eng. 6 (2007) 387–394.
[27] D. Poppendieck, H. Hubbard, M. Ward, C.J. Weschler, R.L. Corsi, Ozone reactions with indoor materials during building disinfection, Atmos. Environ. 41 (2007) 3166–3176.
[28] E. Darling, G.C. Morrison, R.L. Corsi, Passive removal materials for indoor ozone control, Build. Environ. 106 (2016) 33–44.
[29] C.J. Cros, G.C. Morrison, J.A. Siegel, R.L. Corsi, Long-term performance of passive materials for removal of ozone from indoor air, Indoor Air. 22 (2012) 43–53.
[30] G.C. Morrison, W.W. Nazaroff, Ozone interactions with carpet: Secondary emissions of aldehydes, Environ. Sci. Technol. 36 (2002) 2185–2192.
[31] H. Wang, G.C. Morrison, Ozone-initiated secondary emission rates of aldehydes from indoor surfaces in four homes, Environ. Sci. Technol. 40 (2006) 5263–5268.
[32] H. Wang, G.C. Morrison, Ozone-surface reactions in five homes: Surface reaction probabilities, aldehyde yields, and trends, Indoor Air. 20 (2010) 224–234.
[33] J.G. Klenø, P.A. Clausen, C.J. Weschler, P. Wolkoff, Determination of Ozone Removal Rates by Selected Building Products Using the FLEC Emission Cell, Environ. Sci. Technol. 35 (2001) 2548–2553.